

SUPPORTING INFORMATION

Photocatalytic and Photocurrent Responses to Visible Light of the Lone-Pair-Based Oxysulfide $\text{Sr}_6\text{Cd}_2\text{Sb}_6\text{S}_{10}\text{O}_7$

Sandy Al Bacha^{a,b,c}, Sébastien Saitzek^a, Emma E. McCabe^{c*}, Houria Kabbour^{a*}

^a Univ. Lille, CNRS, Centrale Lille, ENSCL, Univ. Artois, UMR 8181 – UCCS – Unité de Catalyse et Chimie du Solide, F-59000 Lille, France

^b University of Kent, School of Physical Sciences, Canterbury, Kent CT2 7NH, U.K

^c Durham University, Departement of Physics, Durham DH1 3LE, U.K.

Corresponding authors: emma.mccabe@durham.ac.uk , houria.kabbour@univ-lille.fr

Stereochemical activity. To quantify the stereochemical activity of the antimony lone pair Sb^{3+} $5s^2$ in the three different entities within the structure, the approach described by *Hu et al.*¹ was adopted. This involves a stereochemical activity ratio calculation based on a simple comparison of the *s* and *p* states of the Sb cation near the Fermi level. The filled antibonding interactions between Sb $5s$ and S $3p$ and/or O $2p$ states (figure S1) is responsible for the stereoactive lone pair (as the revised lone pair model indicates)^{2,3} and is located close to the top of the valence band. Using the following equation:

$$R_{SCA} = I(\text{Sb}-s)/I(\text{Sb}-p) \quad (1)$$

where R_{SCA} is ratio of Sb-*s* states to Sb-*p* states, and $I(\text{Sb}-s)/I(\text{Sb}-p)$ is the integrated PDOS from a specified energy level (point where the intensity of Sb-*s* and Sb-*p* is equivalent) to the Fermi level (figure S2), R_{SCA} was calculated for $\text{Sb}(1)\text{S}_5$, $\text{Sb}(2)\text{S}_4\text{O}$ and $\text{Sb}(3)\text{O}_3$ to be 0.57, 0.59 and 0.64, respectively (Table S1). The smaller R_{SCA} is for the Sb fully coordinated by sulfur (0.568) and the bigger one is obtained for the Sb fully coordinated with the oxygen (0.641) (figure S3), consistent with the results obtained from the COHP calculation that showed an increase in the volume and the distance to Sb upon increasing the oxygen ratio.

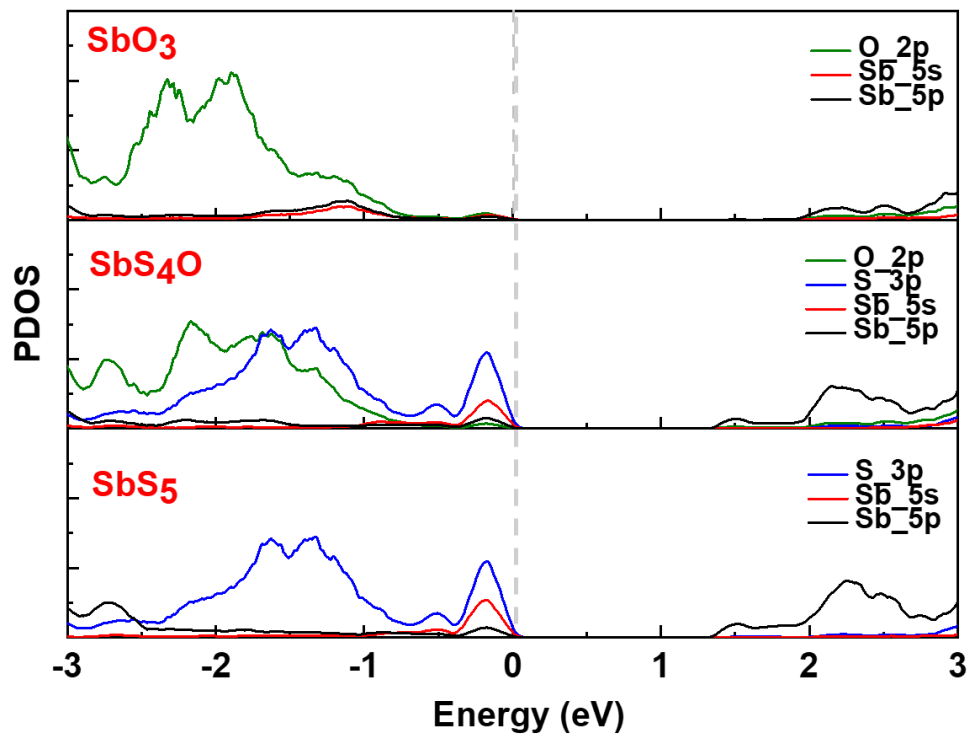


Figure S1: Partial density of states (PDOS) (a) of Sb(3)O₃ and (b) of Sb(2)S₄O and (c) of Sb(1)S₅.

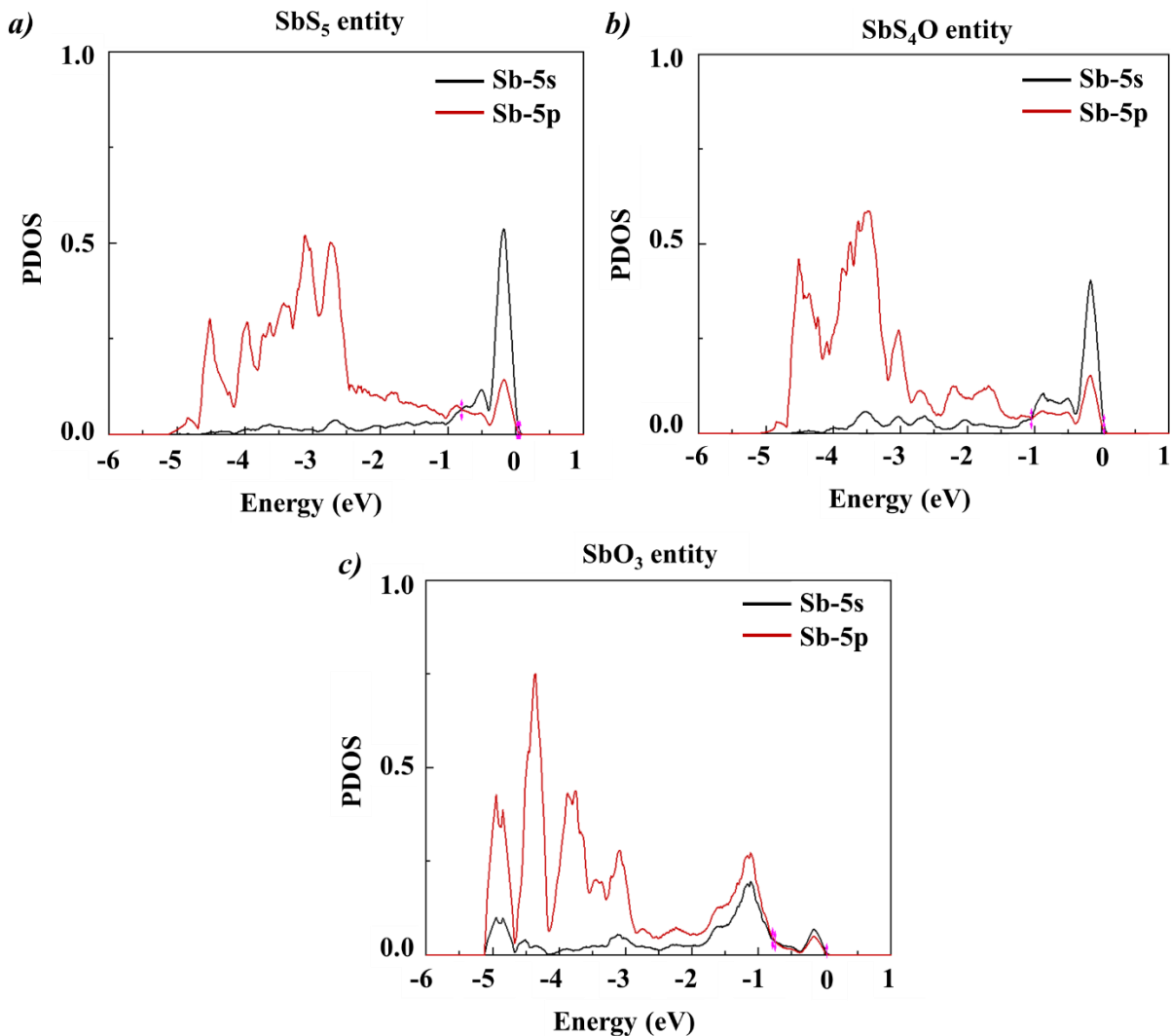


Figure S2: Comparison of PDOS of Sb-5s and Sb-5p (a) in Sb(1)S₅, (b) in Sb(2)S₄O and (c) in Sb(3)O₃ entities.

Table S1. Integrated PDOS from a specified energy level to the fermi level and the calculated stereochemical activity factor for different antimony entities.

	Sb(1)S ₅ _Entity	Sb(2)S ₄ O_Entity	Sb(3)O ₃ _Entity
I(Sb-s)	1.40	1.39	1.28
I(Sb-p)	2.46	2.35	1.99
R _{SCA}	0.57	0.59	0.64

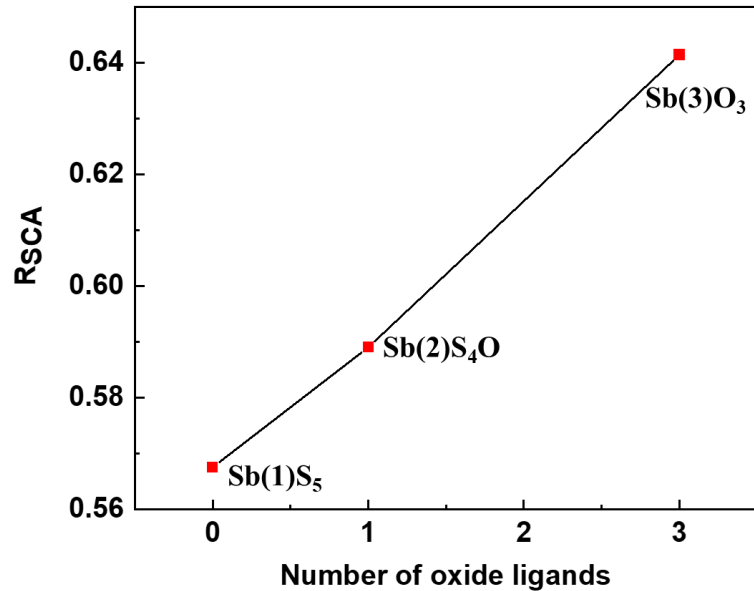


Figure S3: Relationship between stereochemical activity factor R_{SCA} and number of oxide ligands

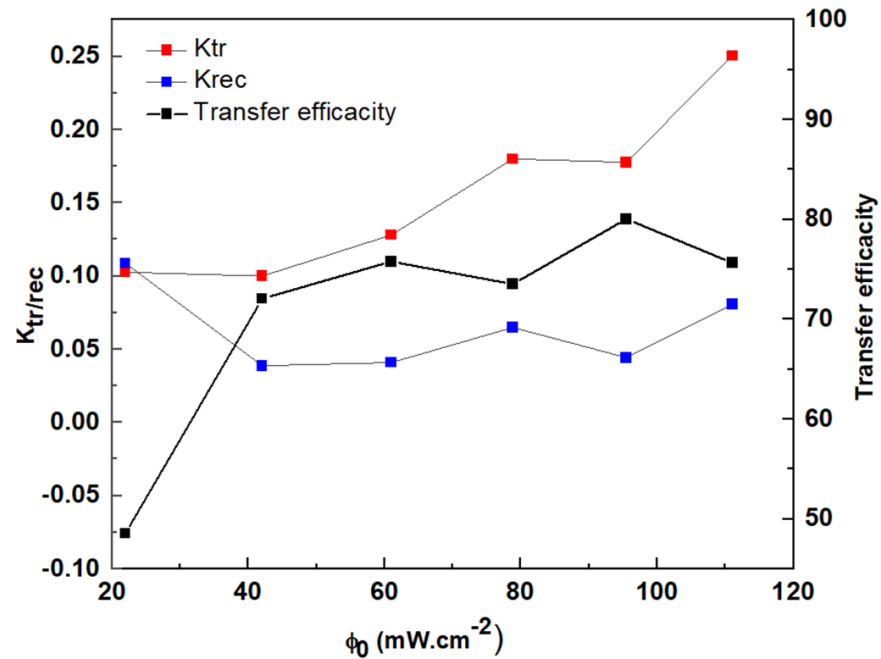


Figure S4: Evolution of the recombination and transfer rate constants k_{tr} and k_{rec} with intensity of light alongside the transfer efficacy η_k by intensity light.

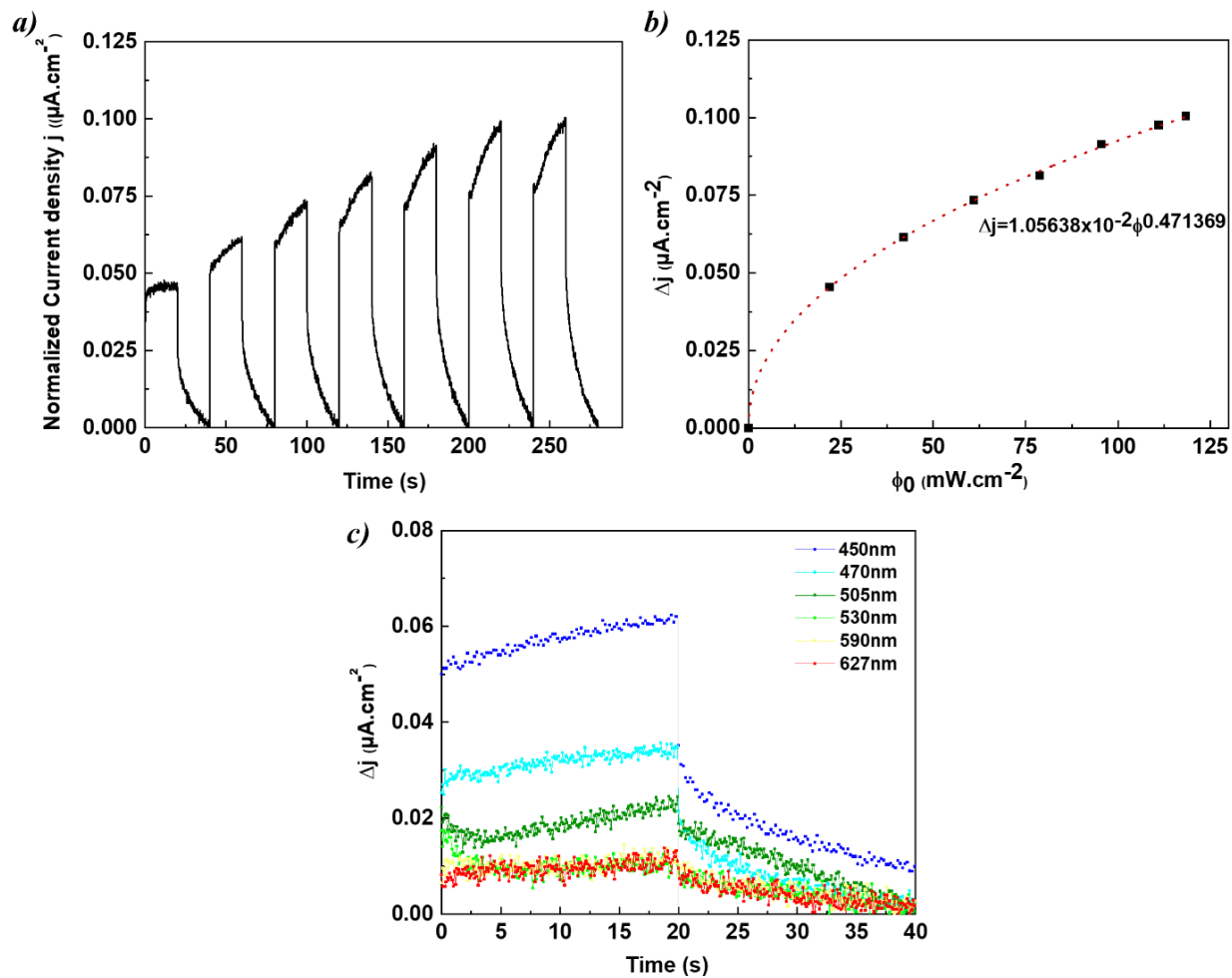


Figure S5: (a) Transient photocurrent response ($V_{\text{bias}}=0$ V under a 450 nm excitation) of $\text{Sr}_6\text{Cd}_2\text{Sb}_6\text{S}_{10}\text{O}_7$ (b) Evolution of the photocurrent density the power density of light (c) Transient photocurrent response vs. wavelengths at a $V_{\text{bias}}=0$ V (constant light intensity $\phi_0=42 \text{ mW cm}^{-2}$) of $\text{Sr}_6\text{Cd}_2\text{Sb}_6\text{S}_{10}\text{O}_7$

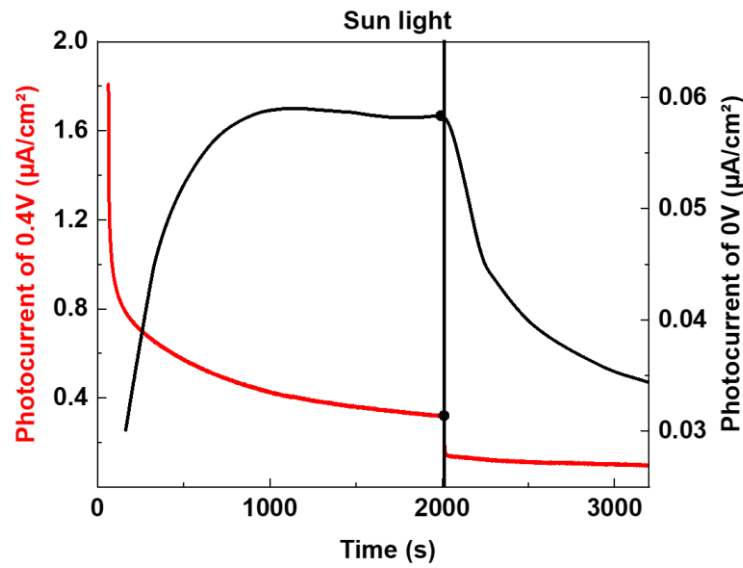


Figure S6: Current density variation at 0V and 0.4V under solar light excitation and a 3200s exposure time.

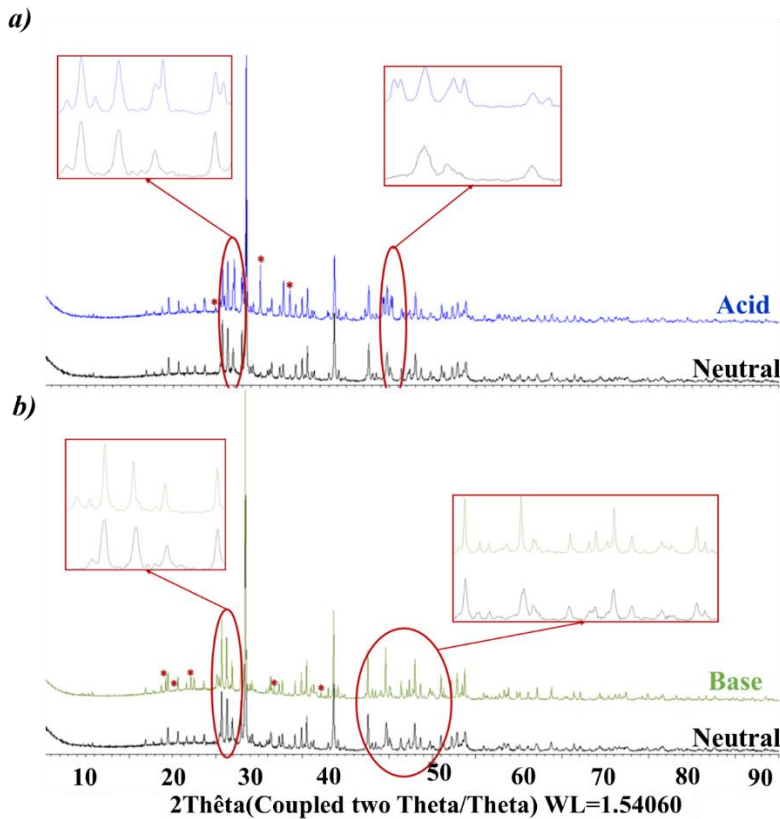


Figure S7: (a) Collected X-ray powder diffraction (XRPD) data of dried powder of $\text{Sr}_6\text{Cd}_2\text{Sb}_6\text{S}_{10}\text{O}_7$ after being in an acid and neutral pH. (b) Collected X-ray powder diffraction (XRPD) data of dried powder of $\text{Sr}_6\text{Cd}_2\text{Sb}_6\text{S}_{10}\text{O}_7$ after being in a basic and neutral pH.

Table S2. Refinement details from Rietveld refinement of $\text{Sr}_6\text{Cd}_2\text{Sb}_6\text{S}_{10}\text{O}_7$ using room temperature XRPD data in space group Cm ; cell parameters are $a = 18.9711(7)$ Å, $b = 4.0544(1)$ Å, $c = 10.0420(3)$ Å, $\beta = 114.871(1)^\circ$; $R_{\text{exp}} = 4.390\%$, $R_{\text{wp}} = 7.062\%$, $R_{\text{p}} = 5.196\%$, $\chi^2 = 3.217$.

Atom	Wyckoff site	x	y	z	$U_{\text{iso}} \times 100(\text{\AA}^2)$	Site occupancy
Sb1	2a	0.3925(5)	0	0.0310(9)	1.5 (1)	1
Sb2	2a	0.2952(4)	0	0.5674(8)	1.5 (1)	1
Sb3	2a	0.4752(4)	0	0.5229(7)	1.5 (1)	1
Cd1	2a	0.2546(3)	0.5	0.1516(5)	0.01(32)	1
Sr1	2a	0.6773(5)	0	0.727(1)	0.3(1)	1
Sr2	2a	0.5343(6)	0.5	0.871(1)	0.3(1)	1
Sr3	2a	0.5859(5)	0.5	0.3550(9)	0.3(1)	1
S1	2a	0.365(2)	0.5	0.815(3)	1.1(3)	1
S2	2a	0.410(2)	0.5	0.223(3)	1.1(3)	1
S3	2a	0.534(1)	0	0.101(2)	1.1(3)	1
S4	2a	0.205(1)	0	-0.014(3)	1.1(3)	1
S5	2a	0.223(1)	0.5	0.377(2)	1.1(3)	1
O1	2a	0.570(3)	0	0.474(6)	1.2(8)	1
O2	2a	0.204(3)	0	0.623(6)	1.2(8)	1
O3	2a	0.551(3)	0	0.734(4)	1.2(8)	1
O4	2a	0.492(5)	0.5	0.582(9)	1.2(8)	0.5

Table S3. Atomic positions of the optimized supercell $a \times 2b \times c$ structure of $\text{Sr}_6\text{Cd}_2\text{Sb}_6\text{S}_{10}\text{O}_7$ given here for $P1$ (the space group of the supercell is Pc). Optimized cell parameters are $a = 19.2631$ Å, $b = 8.10615$ Å, $c = 10.1812$ Å, $\beta = 115.26^\circ$ and $V = 1437.77$ Å³.

Atom	Wyckoff site	x/a	y/b	z/c
Sb1	1a	0.39384	0.00021	0.03020
Sb2	1a	0.89384	0.24979	0.03020
Sb3	1a	0.39356	0.49981	0.03007
Sb4	1a	0.89356	0.75020	0.03007
Sb5	1a	0.30024	0.00055	0.58288
Sb6	1a	0.80024	0.24945	0.58288
Sb7	1a	0.30110	0.49951	0.58275
Sb8	1a	0.80110	0.75049	0.58275
Sb9	1a	0.47983	0.01058	0.52718
Sb10	1a	0.97983	0.23942	0.52718
Sb11	1a	0.47983	0.48938	0.52712
Sb12	1a	0.97983	0.76062	0.52712
Sr1	1a	0.68064	-0.00224	0.72998
Sr2	1a	0.18064	0.25224	0.72998
Sr3	1a	0.68075	0.50224	0.72993
Sr4	1a	0.18075	0.74776	0.72993
Sr5	1a	0.53344	0.25010	0.85904
Sr6	1a	0.03344	-0.00010	0.85904
Sr7	1a	0.53860	0.74988	0.88701
Sr8	1a	0.03860	0.50012	0.88701
Sr9	1a	0.59223	0.25007	0.35837
Sr10	1a	0.09223	-0.00007	0.35837
Sr11	1a	0.59267	0.74992	0.35457
Sr12	1a	0.09267	0.50008	0.35457
Cd1	1a	0.25844	0.24841	0.15751
Cd2	1a	0.75845	0.00159	0.15751
Cd3	1a	0.25938	0.75156	0.15867
Cd4	1a	0.075938	0.49844	0.15867
S1	1a	0.35986	0.25059	0.79427

S2	<i>1a</i>	0.85986	-0.00059	0.79427
S3	<i>1a</i>	0.36119	0.74940	0.79546
S4	<i>1a</i>	0.86119	0.50060	0.79546
S5	<i>1a</i>	0.40576	0.24907	0.21362
S6	<i>1a</i>	0.90576	0.00093	0.21362
S7	<i>1a</i>	0.40692	0.75083	0.21076
S8	<i>1a</i>	0.90692	0.49917	0.21076
S9	<i>1a</i>	0.53255	0.00659	0.09505
S10	<i>1a</i>	0.03255	0.24341	0.09505
S11	<i>1a</i>	0.53256	0.49344	0.09531
S12	<i>1a</i>	0.03256	0.75656	0.09531
S13	<i>1a</i>	0.20704	-0.00036	0.98480
S14	<i>1a</i>	0.70704	0.25036	0.98480
S15	<i>1a</i>	0.21073	0.50038	0.98989
S16	<i>1a</i>	0.71073	0.74962	0.98989
S17	<i>1a</i>	0.23221	0.24973	0.38208
S18	<i>1a</i>	0.73221	0.00027	0.38208
S19	<i>1a</i>	0.23265	0.75028	0.38256
S20	<i>1a</i>	0.73265	0.49972	0.38256
O1	<i>1a</i>	0.56741	-0.00308	0.47685
O2	<i>1a</i>	0.06741	0.25308	0.47685
O3	<i>1a</i>	0.56740	0.50307	0.47678
O4	<i>1a</i>	0.06740	0.74693	0.47678
O5	<i>1a</i>	0.20619	-0.00008	0.61344
O6	<i>1a</i>	0.70619	0.25008	0.61344
O7	<i>1a</i>	0.20665	0.50009	0.61204
O8	<i>1a</i>	0.70665	0.74991	0.61204
O9	<i>1a</i>	0.54554	-0.02642	0.73671
O10	<i>1a</i>	0.04554	0.27642	0.73671
O11	<i>1a</i>	0.54549	0.52645	0.73656
O12	<i>1a</i>	0.04549	0.72355	0.73656
O13	<i>1a</i>	0.49246	0.25002	0.58319
O14	<i>1a</i>	0.99246	-0.00002	0.58319

REFERENCES

- (1) Hu, C.; Mutailipu, M.; Wang, Y.; Guo, F.; Yang, Z.; Pan, S. The Activity of Lone Pair Contributing to SHG Response in Bismuth Borates: A Combination Investigation from Experiment and DFT Calculation. *Physical Chemistry Chemical Physics* **2017**, *19* (37), 25270–25276.
- (2) Payne, D. J.; Egddell, R. G.; Walsh, A.; Watson, G. W.; Guo, J.; Glans, P.-A.; Learmonth, T.; Smith, K. E. Electronic Origins of Structural Distortions in Post-Transition Metal Oxides: Experimental and Theoretical Evidence for a Revision of the Lone Pair Model. *Physical review letters* **2006**, *96* (15), 157403.
- (3) Walsh, A.; Payne, D. J.; Egddell, R. G.; Watson, G. W. Stereochemistry of Post-Transition Metal Oxides: Revision of the Classical Lone Pair Model. *Chemical Society Reviews* **2011**, *40* (9), 4455–4463.